A Numerical study of compacted clay tensile strength by discrete element modelling: A bending test application

A Ammeri, M Jamei, H Guiras, M Bouassida, P Villard, O Plé, S Camp, Jean-Pierre Gourc

A Numerical study of compacted clay tensile strength by discrete element modelling: A bending test application

A. Ammeri*, M. Jamei, H. Guiras**, M. Bouassida***
** Civil Engineering Laboratory,* Geotechnical Engineering,
National Engineering Scholl of Tunis (ENIT)
E-mail: mehrez.jamei@enit.rnu.tn
**Corresponding author

P. Villard , O. Plé, S. Camp, J.P Gourc
Laboratoire Interdisciplinaire de Recherches impliquant la Géologie et la Mécanique de Grenoble (LIRIGM),
University Joseph Fourier of Grenoble, France

Abstract: The study of the clay tensile behaviour is one of the topics which require a specific lighting especially when we give a closely attention to the pathology of the works built with or on the clays submitted to significant tensile strength. Therefore, failure or damage of clay can be related especially to tensile limit and not to shear limit overtaking. It is the case of compacted clay liners in wastes landfill cover or for embankments built on high compressible soils. In order to study the tensile compacted clay behaviour, a series of laboratory bending tests were carried out. On the basis of the test results, different numerical simulations using Discrete Element Method were engaged. Two numerical bending tests were carried out: a three points bending and a four points bending. A comparison between the two numerical protocols is given. Four analytical models (classical elasticity, bimodular elasticity, differential model and struts-tie method) are used in order to interpret bending tests results and are compared with the numerical simulations. At the same time, the validity of the assumptions relative to the four models was discussed. To lead to these results, a study and adjustment of numerical and micromechanical parameters were carried out. It was demonstrated that the Discrete Element Method has a strong correlation with a laboratory tests and can contribute somewhat to the understanding and discussion on the validity degree of the kind of indirect tests and of their interpretation.

Keywords: tensile strength; bending test; Discrete Elements Method; tensile failure; analytical model.

1 INTRODUCTION

The compression behaviour study of clay soils was largely investigated. Indeed, by the confined compression tests, various behaviour laws are proposed and validated. The post-failure and the bifurcation phenomenon were also well studied.

However, the tensile clay behaviour is poorly studied. Indeed, only few aspects of the clay behaviour are investigated such as the reliable experimental procedure to determine the tensile elastic parameters and even less the failure such the limit tensile strength.

Moreover, the behaviour of rigid materials such as a rocks and a concrete, under tensile load conditions was relatively well established, although, the question to find an efficient experimental protocol leading to reliable tensile strength is not completely resolved.

For example for rock materials; according to different authors (Cai and al., 2004; Claesson and al., 2002; Manoj and al., 2005) the recourse to indirect tensile (such flat brazilian test or beam test) is often necessary and the direct tension test is not commonly conducted in laboratory.

According to several flatten and classical Brazilian tests' results, various conclusions on the rocks (Kaklis and al., 2005) or on the concrete (Manoj and al., 2005) have been noted. The first one is that, the indirect tensile test is simple and it can lead to have a convenient tensile strength only if the initiation of cracking is localised at the centre of the sample. The major disadvantage related to the test is that the shear stresses induced at the vicinity of the loading platens prevents the tensile stresses to develop. Second, the difficulty is to have a convenient model in order to have reliable tensile characteristics. Indeed, the bimodular elasticity behaviour must be considered: i.e. tensile and compression rigidities are different. And the homogenous tensile zone at the centre must be required for determining the true strain-stress characteristics of soil. For some authors this latter condition is related to the dimension of the critical loading angle, which corresponds to the flat ends (Q Z Wang and al., 2004).

Another alternative indirect test was used, like the bending beam tests, which is easily to carry on in particular on

compact materials. Unfortunately, it remains depending on the experimental protocol and on interpretation method. Indeed, the results depend on the sample dimensions, on the sample shape and on the type of the bending beam test (3 points or 4 points bending tests) (Satyanrayana and al. 1972).

The relevance of the interpretation of this test depends on its instrumentation, in particular the stress measurement and the corresponded strains at the tensile zones. The tensile failure deduced from bending tests depends on the assumptions validity of the models (Ajaz, A. and al., 1975)

In conclusion, for rocks or for concrete, all the difficulties are related to indirect tests interpretation. They are more significant for the clay soils and are more and more important for the water content increasing (Addanki and al., 1974).

Due to the experimental and theoretical analysis difficulties, alternative numerical technique was developed in order to determine the tensile strength and to examine the several proposal analytical models for the bending tests.

The Distinct Element Method (DEM) was calibrated with direct compressive tests and applied to bending beam tests. This paper describes the experimental protocol and the numerical approach calibration.

Basing on numerical bending tests, a comparison between three points bending and four points bending results was done. This comparison between the two numerical protocols must lead to conclude about the basic difference.

2 A BENDING EXPERIMENTAL PROTOCOL

Experimental tests were carried out in Lirigm laboratory with a plastic clay soil provided from l'Aptien region and with the following characteristics:

Physical Characteristics:	Mechanical Characteristics:
Kaolinite: 50%, Illite: 40%	Undrained friction angle= ϕ_u=24°
% < 2 µm : 50 %	Undrained cohesion= 30kPa
% 2 µm until 80 µm: 48 %	IPI = 11 – 12
Dry density = 21 kN/m^3, Ip= 24%, void ratio=0,56	Permeability = 10^{-9} m/s - 10^{-11} m/s

Table 1: Physical and mechanical clay characteristics

The four bending tests were selected and conducted with field displacement measurements by two ways. The first way corresponds to a three displacement transducers which are used; two are placed on the two support rods, the third is placed in the middle of specimen. The second way (for which the results are not presented in the paper) corresponds to the post-graphic technique using a software treatment.
Figure 1 shows the beam test carried on a sample of 10 cm x 10 cm x 40 cm and the cracking mode. The tensile crack thickness is more important at the bottom and it is developed progressively to the top of the specimen. This indicates that the failure is essentially localised in tensile zone at the bottom of the beam. In order to keep a same initial conditions like the water content and the dry density, the Proctor optimum parameters are fixed (the initial water content is near the 16%= optimum water content + 2%). *Figure 7* shows the force-displacement curve. Unfortunately, it was difficult to have at same time exactly initial water content and initial density for each test. Consequently, the little water content variation was notified and it effect was estimated (*figure 7*).

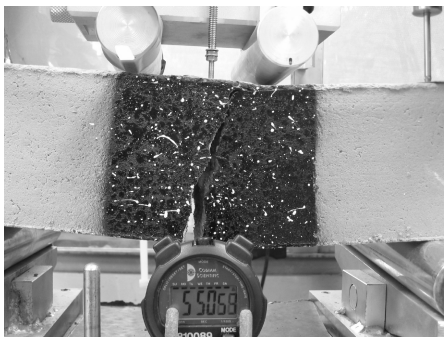

Figure 1: Beam test and cracking mode

According to the whole of the experimental results, numerical simulations of the bending test were carried out and some micro-mechanics parameters are calibrated on different experimental compression and bending tests. The calibration is illustrated in the section 3.2.

3 A DISCRETE ELEMENT APPROACH FRAMEWORK

3.1 A principal of DEM approach

In the last few years the Discrete Element Method is one of the emerging numerical techniques used to investigate the failure and the fracture behaviour of complex testing materials. The interest of this approach is to consider simple individual laws for contacts between the particles. For the numerical software used (PFC^{2D}), these laws relate the relative displacement with contact forces and rigidities (1),(3):

$$F_i^n(t)=K^n U_i^n(t) n_i \quad (1)$$

$$\Delta F_i^s=-K^s \Delta U_i^s \quad (2)$$

$$F_i^s(t)=F_i^s(t-1)+\Delta F_i^s \quad (3)$$

Where: F_i^n and F_i^s are respectively the normal and tangential forces in contact (i) between two particles with normal n_i, and U_i^n and ΔU_i^s the normal and relative tangential displacements in contact (i). Also (t) is a time step in the particle movement.

The distinct element scheme is based on the second Newton law of motion. Force displacement law at contact for the translation motion (4) and moment-rotational moment relation for the rotation motion (5).

$$F_i=m_i(\ddot{x}_i-g_i) \quad (4)$$

$$M_{i(3)}=I_{i(3)}\dot{\omega}_{i(3)} \quad (5)$$

Where: m_j is the particle's mass, $\ddot{x}_i$ the acceleration, g_i the volumetric gravity force of particle (i), $M_{i(3)}$, $I_{i(3)}$ and $\dot{\omega}_{i(3)}$ respectively the resultant moment, the principal moment of inertia of the particle and the angular acceleration about the principal axe 3.

The contacts are defined by five rheological parameters: normal and tangential stiffnesses (K^n and K^s), normal and shear cohesions (C^n and C^s) and friction coefficient (μ). It assumed that the parameters of the two contacting partners act in series (*figure 2*). With the micromechanics parameters the real contact condition between all particles are adjusted step by step. And all reliable contacts are re-actualized according to these two conditions (6) and (7).

$$\left|F^s\right| \geq F^s_{\max} \tag{6}$$

$$F^n \geq C^n \tag{7}$$

$$F^s_{\max} = \max(\mu \left|F^n\right|, C^n) \tag{8}$$

The major difficulty to use this approach for real application is to assign the good micro-properties to have the true relationship between micro-properties and macro-properties. A preliminary parametrical numerical study is needed in order to fit the micro-parameter.

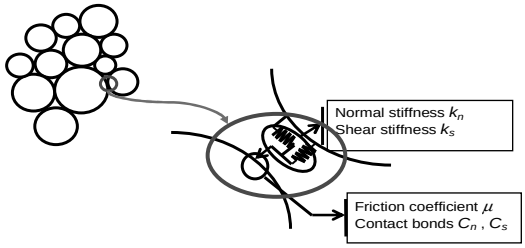

Figure 2: A rheological model on the DEM method

3.2 The micro-macro relationship in the simulation approach

The fitting between the micro and macro parameters is made by carrying out various numerical direct compressive tests. In this case, the macro- homogeneity condition is traduced by the good prediction of the experimental curve. *Figure 3* shows the results of an experimental prediction of unconfined compression tests. The experimental curve corresponds to the average tests data.

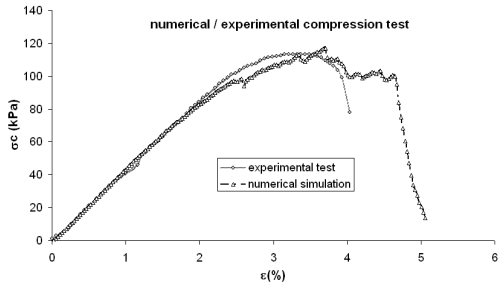

Figure 3: An experimental prediction of unconfined compression

For all following simulation tests the retained micro-mechanical properties of the Discrete Element Method are: the normal and shear stiffness K_n =K_s= 14 MN/m; the friction coefficient μ = 0.8; the normal and shear bonds C^n and C^s defined as:

$$C^n = C_f{}^n \min(rad(b_i), rad(b_j)) \tag{9}$$

And $$C^s = C_f{}^s \min(rad(b_i), rad(b_j)) \tag{10}$$

Where $C_f{}^n = C_f{}^s$ =300 kN/m ; rad(b_i) and rad(b_j) are the radius of the two balls (i) and (j) acting in the contact (in two-dimensional problem the balls are considered as cylinders).

4 EVALUATION OF NUMERICAL AND EXPERIMENTAL RESULTS

To illustrate how the numerical approach has a great potentiality to predict the indirect test results, several numerical tests in different conditions are carried out. Systematic comparison between numerical and experimental results with a qualitative and a quantitative analysis is given. *Figure 4* shows the identical failure mechanisms between experimental and numerical results of direct compressive tests and improves how the DEM approach can reproduces perfectly the sliding mode.

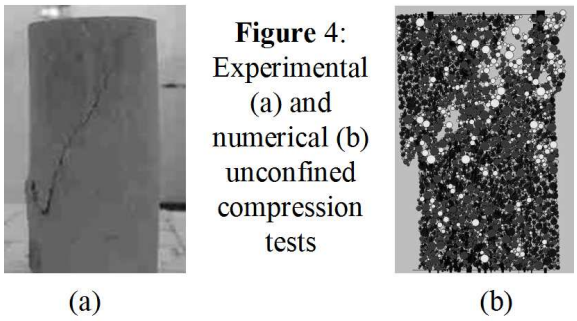

Figure 4: Experimental (a) and numerical (b) unconfined compression tests

(a) (b)

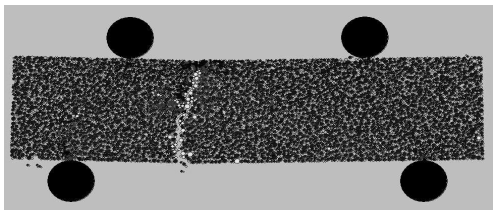

Figure 5: Numerical bending test failure

Figure 5 shows similarly failure mode with its experimental equivalent bending test (*figure 1*). The difference between the x-coordinate failure sections between experimental and numerical is not significant while deflexion moment is constant between the two rods for transferring loads. The quantitative results are illustrated in the *figure 7*.

In general it is admitted that for the validity of the essential assumptions of the beam's theory, the twinge must be greater than 10. However, for the clay soil the bending experimental system is designed for low twinges (2-4,5). Hence, in order to quantify the effect of low twinge on the interpretation of the laboratory bending tests, a numerical study has been done with several twinge values. *Figure 6* shows that the effect of the beam's twinge is not significant on limit tensile strength calculated with elastic theory.

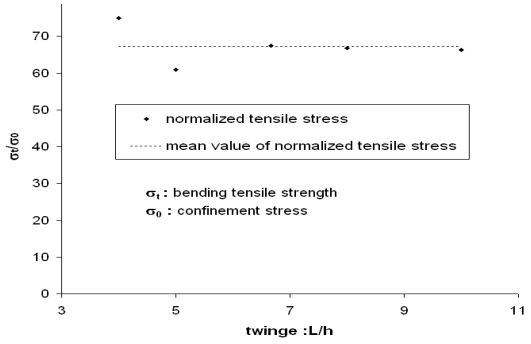

Figure 6: effect of twinge of the sample in bending test

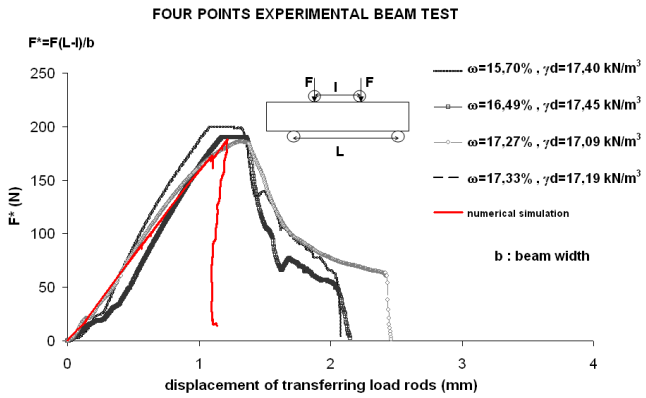

Figure 7: Experimental and Numerical bending tests simulations

As shown in *figure 7*, the reproducibility of experimental tests is conditioned by the possibility to keep the value of the initial water content to a constant. This condition remains difficult and usually conducts to repeat the experience many times.

In conclusion the DEM approach leads with practical way to predict different bending beam tests with different initial conditions. Indeed, it allows simulating the effect of twinge of specimen and the experimental protocol effects. We also demonstrate that if the calibration of the micro-parameters is well established this numerical scheme can enable indirect or direct tensile computation. Basing on the numerical tests, this approach is a convenient tool to give an accurate interpretation of the experience and can be used to examine and to improve a convenient model.

5 ANALYSIS OF DIFFERENT MODELS WITH THE DEM RESULTS

Numerous analytical models were used in order to interpret the bending tests. For some authors (Ajaz, A. and al., 1975), the bending tests (for three or four points system) results can not be analysed in the elastic theory framework. The no validity of the theory was attributed to bi-modularity behaviour (Stimpson, B., Rui Chen, 1993). In this case, the use of identical stiffness values for tension and compression analysis of clay structure is not justified (Ajaz, A. and al., 1974). In order, to verify this property an investigation in terms of total stress is concerned with both stress-strain behaviour and limit strength condition which leads to limit strength diagram (*figure 10*).

5.1 Four points bending system

In the section all comparisons are given for the σ_{xx} stress, which is defined as a normal stress to the vertical section. It has been positive in compression and negative in tensile.

5.1.1 Numerical calculation

The numerical calculation of σ_{xx} stress is given by equation (11). Indeed, σ_{xx} stress values are calculated using the discrete-particles efforts according (11) by the measurement circles (*figure 8*):

$$\bar{\sigma}_{ij} = -\left(\frac{1-n}{\sum_{N_p} V^{(p)}} \right) \sum_{N_p} \sum_{N_c} \left| x_i^{(c)} - x_i^{(p)} \right| n_i^{(c,p)} F_j^{(c)} \qquad (11)$$

Where the summations are taken over the N_p balls with centroids contained within the measurement circle in the specimen and over the N_c contacts of these balls.

- n is the porosity within the measurement circle;
- $V^{(p)}$ is the volume of particle (p), taken equal to the area of particle (p) times a unit-thickness;
- $x_i^{(p)}$ *and* $x_i^{(c)}$ are the locations of a particle centroid and its contact, respectively;
- $n_i^{(c,p)}$ is the unit normal vector directed from a particle centroid to its contact location;
- $F_j^{(c)}$ is the force acting at contact (c)

In order to assure the convenient failure stress computation, different sections are considered in area comprising between the two points for transferring load. *Figure 9* shows the stress field homogeneity and the independence of choice of x-coordinate of section in this area.

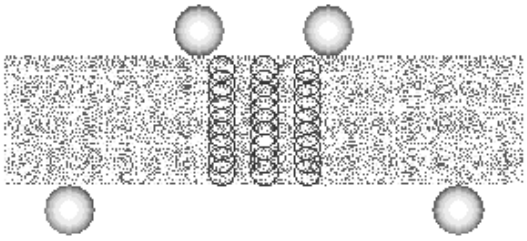

Figure 8: positions of measurement circles

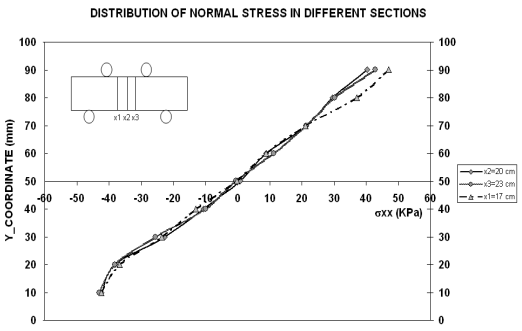

Figure 9: Normal stress curves in different sections

If a mono-modularity elasticity model is applied, the tensile stress is calculated as in equation (12). Where in this equation σ_{xx} is the tensile and the compression stress at top and at bottom of the beam. *Figure 10* shows that equality between the normal compression and tensile stress (designed stress by the equation (12)) is not justified and that the difference between the two values increases with strain. Hence, it leads to conclude that at failure the compressive strength of clay is higher than the tensile strength. At failure the stress diagram differs from the tension curves obtained by the standard elastic bending theory. For Troloppe D. L., and Chan, C. K. (1960), the considerably irregular stress-strain behaviour for compacted clay was also observed.

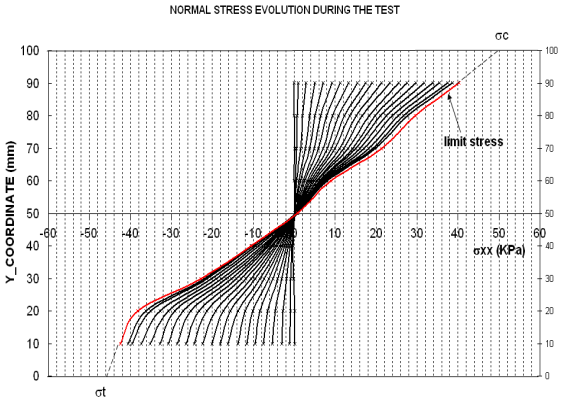

Figure10: Numerical Tensile and compressive stress curves

For each loads which are applied incrementally, the non linearity tensile stress diagram increases with loading and in extreme tensile fibre. It seems that the numerical results improve the stress diagram obtained by differential method (Ajaz, A. and Parry; R. H. G., 1975,-b-). Nevertheless, the other bending theories (which are presented following briefly) use other formulations of the compression and tensile stresses. The aim in this section is to compare between the numerical simulations and the models' results.

5.1.2 The elastic bending method

The elastic bending theory method leads to equation (12) which based on the assumption that the Young's modulus has the same value for the material in tension as in compression:

$$\sigma_{c,t}=\frac{6M}{bh^2} \tag{12}$$

Where M is the flexion moment, b and h are the width and the height of the plane section.

5.1.3. The Bimodular elasticity method (Ajaz, A. and Parry; R. H. G. , 1975,-b-).

The method is based on all the same assumptions of the elastic bending method, but the value of deformation modulus in tension may differ from that in compression. It leads to equation (13-a) and (13-b):

$$\sigma_c=\frac{3M}{bh^2}\frac{\varepsilon_c+\varepsilon_t}{\varepsilon_c} \tag{13-a}$$

$$\sigma_t=\frac{3M}{bh^2}\frac{\varepsilon_c+\varepsilon_t}{\varepsilon_t} \tag{13-b}$$

Where ε_c and ε_t are respectively the compression strain at top and the tensile strain at bottom of the beam. In this case, the compression and the tensile modulus are E_c=25MPa and E_t= 44MPa.

5.1.4. The Differential method (Ajaz, A. and Parry; R. H. G. , 1975,-a- and -b-).

In opposition to the two previous methods, this model does not assume a preferred relationship between stress and strain. Indeed, the behaviour law is unknown. The model leads to equations (14-a) and (14-b).

$$\sigma_c=\frac{1}{\varepsilon_c+\varepsilon_t}\frac{\partial}{\partial\varepsilon_c}\left[\frac{M(\varepsilon_c+\varepsilon_t)^2}{bh^2}\right] \tag{14-a}$$

$$\sigma_t=\frac{1}{\varepsilon_c+\varepsilon_t}\frac{\partial}{\partial\varepsilon_t}\left[\frac{M(\varepsilon_c+\varepsilon_t)^2}{bh^2}\right] \tag{14-b}$$

Hence, the compression and tensile stress are calculated by the differentiating the quantity $M(\varepsilon_c+\varepsilon_t)^2$ with respect ε_c and ε_t. It is evidently, that the compression and tensile stress values are calculated respectively with (14-a) at the top of the bending sample and with (14-b) at its bottom. We make in the numerical calculations the assumption that b and h (beam dimensions) are constant.

5.1.5. Comparison between the numerical and analytical methods

The table 2 summarizes the results of numerical and the three analytical models. It appears that the numerical and

bimodular models give almost the same value of compression stress. Nevertheless, the tensile stress obtained by the numerical and elastic theory is lower than those obtained by the other methods. Hence, it is difficult to conclude about the efficiency of the allowed assumptions of the analytical models. The use of direct test and probably another indirect tests (like Brazilian tests) can help to give a clearly conclusions.

	Numerical	Bimodular	Elastic theory	Differential method
σ_c(kPa)	45.00	47.42	53.92	53.95
σ_t(kPa)	50.00	62.46	53.92	68.34

Table 2: Compression and tensile stress from different models

5.2 Three points bending system

In order to study the validity of struts-tie model (J. C. Morel and al., 2003), a numerical simulations by the DEM method have been done. Therefore, in the section, we present only numerical results corresponding to the three points bending tests.

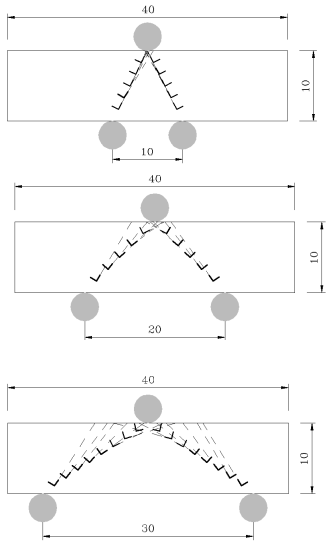

Figure 11: principal stresses orientation in struts zone (figures 11-a, 11-b and 11-c)

The *figure 11* shows that basing to the principal stresses distribution the validity of struts-tie method is improved only until a limit distance between the tow support rods. Indeed, in order to interpret the behaviour at failure of a compressed earth block during a three points bending test, the struts-tie method was proposed by J. C. Morel and al. (2003) which suppose that it is possible to deduce the tensile strength via the compression stress value developed in the struts. Hence, from numerical results it appears that modelling the three points bending system as a lattice is valid only for limited distance between the tow support rods (figure 11-a). The orientation of the principal stresses improves this conclusion. Indeed, it is shown on figure 11 that the compression direction as a lattice is not possible if the distance between the two support rods increases (figures 11-b and 11-c).

6 CONCLUSION

The numerical study carried out with the PFC^{2D} code improves the potential of this method which can take the place of many experimental tests. The comparison between the four models improves also the validity of this method to predict the macroscopic behaviour and leads to the study of the limit tensile strength. The limitation of the elasticity method to predict the failure tensile strength was also improved. It seems that the differential method conducts to the same numerical tensile stress diagram. Indeed, the differential method is chosen for comparison because it is not based on a preferred behaviour law assumption.
The numerical simulations improve the bimodular elasticity behaviour. Our future work also includes exploiting numerical Brazilian and direct tensile tests to improve the ability of the DEM analysis to give a quantified limit tensile strength of the compacted clay.

REFERENCES

Addanki V. Gopala Krishnayya, Zdenek Eisenstein and Nobert R. Morgenstren (1974;) 'Behaviour of Compacted Soil in Tension'. J. of the Geotechnical Engineering Division, september, pp. 1050-1061.

Ajaz, A. & Parry; R. H. G. (1974) 'An unconfined direct tension test for compacted clay'. ASTM Jnl Testing and Evaluation **2**: 3, 163-172.

Ajaz, A. & Parry; R. H. G. (1975)-a- 'Stress-strain behaviour of two compacted clays in tension and compression'. Geotechnique **25**, No. 3, 495-512.

Ajaz, A. & Parry; R. H. G. (1975)-b- 'Analysis of bending stresses in soil beams'. Geotechnique **25**, No. 3, 586-591.

Cai M., Kaiser P.K., (2004)'Numerical simulation of the brazilian test and the tensile strength of anisotropic rocks with pre-existing cracks',Int.J. Rock Mech.Min.Sci, Vol. 41, n°3, 1-6.

Claesson J., Bohloli B. (2002) 'Brazilian test: stress field and tensile strength of anisotropic rocks using an analytical solution'. International Journal of Rock Mechanics & Mining Sciences 39, 991-1004

Jean-Claude Morel, Abalo P'kla and Hervé Di-Benedetto (2003) 'Essai in situ sur bloc de terre comprimée'. Revue Française de Génie Civil, Volume 7, n° 2, 221-237.

Kaklis K. N., Agioutantis Z., Sarris E., Pateli A. (2005) 'A theoretical and numerical study of discs with flat edges under diametral compression (Flat Brazilian test)'. 5th GRACM International Congress on Computational Mechanics. Limassol, 29 June-1 July.

Manoj Khanal, Wolfgang Schubert, Jürgen Tomas (2005). 'DEM simulation of diametrical compression test on particle compounds'. Granular Matter. 7: 83-90.

Narain J., Rawat C. (1970) 'Tensile strength of compacted soils'. J. of the soils Mechanics and Foundations Division, Vol. 96, n° SM4, pp. 2185-2190.

Satyanarayana B. and Satyanarayana Rao (1972) 'Measurement of tensile strength of compacted soils' Technical note. Geotechnical Engineering, Vol. 3.

Stimpson, B., Rui Chen (1993) 'Measurement of rock elastic moduli and in compression and its practical significance'. Can. Geotech. J. **30**, 338-347.

Troloppe, D. L., Chan, C. K. (1960), 'Soil structure and step-strain phenomenon'. Jnl Soil Mech. Fdn Div. Am. Soc. Civ. Engrs **86**, SM2, 1-39.

Wang, Q. Z., Jia X. M., Kou S. Q., Zhang Z. X., Lindqvist, P¨.-A., (2004), 'The flattened Brazilian disc specimen used for testing elastic modulus, tensile strength and fracture toughness of brittle rocks: analytical and numerical results', Int. J. Rock Mech. Min. Sc., 41, 245-253.